DOI: 10.24850/j-tyca-2025-04-10

Notes

Design of hydraulic structures in supercritical regime with sediments: A mathematical criterion to calculate bottom roughness

Diseño de estructuras hidráulicas en régimen supercrítico con sedimentos: un criterio matemático para calcular la rugosidad del fondo

Jesús Gracia-Sánchez[1], ORCID: https://orcid.org/0000-0003-2555-0802

Oscar Arturo Fuentes-Mariles[2], ORCID: https://orcid.org/0000-0003-1888-2913

Judith Ramos[3], ORCID: https://orcid.org/0000-0001-9979-977X

[1]Instituto de Ingeniería, UNAM, Mexico City, Mexico, JGraciaS@iingen.unam.mx

[2]Instituto de Ingeniería, UNAM, Mexico City, Mexico, OFuentesM@iingen.unam.mx

[3]Instituto de Ingeniería, UNAM, Mexico City, Mexico, JRamosH@iingen.unam.mx

Corresponding author: Judith Ramos, JRamosH@iingen.unam.mx

Abstract

In some channels with high gradients, heavy scouring and erosion, as well as overflow, is highly common to occur, thus it is required a water flow velocities regulation. An option for achieving this, is to significantly increase the channel's bottom roughness through the installation of rapid hydraulic structures. However, in sedimentary density fluids, the change in velocity generates the deposition of solids which could be consolidated by changing the geometric design of these structures. This study aims to estimate the degree of confidence expected when modifications are made to the artificial roughness geometries at the bottom of the channel with turbulent and sediment flows. This modification requires to transverse the ribs into ramps by using experimental mathematical analysis. The study enables us to conclude that the new generated bottom roughness produces more stable water flows, and t is also a way to reduce flow velocities.

Keywords: Ramp roughness, transverse ribs, rapid hydraulic structure, energy dissipation, sediment deposit.

Resumen

En algunos canales revestidos con pendientes altas es muy común que ocurran fuertes socavaciones y erosión, así como desbordes, por lo que se requiere una regulación de las velocidades del flujo de agua. Una opción para lograrlo es aumentar significativamente la rugosidad del fondo mediante la instalación de estructuras hidráulicas rápidas. Sin embargo, en fluidos con sedimentos, el cambio de velocidad genera la deposición de sólidos, los cuales podrían consolidarse, cambiando el

diseño geométrico de estas estructuras. Este estudio tiene como objetivo estimar el grado de confianza esperado cuando se producen modificaciones en las geometrías de rugosidad artificial en el fondo del canal con flujo turbulento y densidad de fluido. Esta modificación modifica barras transversales en rampas con base en un análisis matemático experimental. El estudio permite concluir que la rugosidad del fondo generada provoca flujos de agua más estables y es una forma de reducir las velocidades de flujo.

Palabras clave: rugosidad de rampa, barras transversales, estructura hidráulica rápida, disipación de energía, depósito de sedimentos.

Received: 17/11/2023

Accepted: 04/06/2024

Available ahead of print: 24/06/2024

Version of record: 01/07/2025

Introduction

Spatial and temporal scale variations in a river imply changes in energy, discharge, velocity, channel characteristics and load from its source to its discharge. These variations define the natural features of the floodplain and the processes of the river, such as erosion, transportation, and deposition of solids through the stream. Processes that respond to any changes in velocity profile shape, since it is affected by the shear stress and the friction either along the bed or liquid interface (between density current and clear water), create a sedimentary density current

(Kashefipour, Daryaee, & Ghomeshi, 2018). In this type of current, the velocity and the depth of the body (thickness of flow) are calculated as the cross-sectional area average value along the river's course. Thus, flow velocity has a determinant role in many fluvial processes and properties, being necessary to consider a fast flow upstream, but slow downstream due to an increase in the cross-section, making the channel broader and deeper (Schneider, Rickenmann, Turowski, & Kirchner, 2015).

In some channels with high gradients, it is being required a water flow velocities regulation that guarantee that flow velocities could not reach values considerably higher than the values established as limits to avoid both sedimentation (minimum velocity) and erosion at the channel bed (maximum velocity) such as: from 0.9 to 1.0 $m{\cdot}s^{-1}$ for clay channels and channels with rock and simple mixture, and 3.0 to 5.0 $m{\cdot}s^{-1}$ for channels covered with concrete (Chanson, 1999; Tollner, 2021). Yochum, Bledsoe, David and Wohl (2012) observed that an average velocity of 0.44 $m{\cdot}s^{-1}$ could be predicted with an average error lower than 0.071 $m{\cdot}s^{-1}$ when discharge and bedform geometry are known, and 0.10 $m{\cdot}s^{-1}$ (23 %) when only bedform geometry is identified. Also, Ferguson (2022) noted that as many natural reaches are non-uniform, the cross section varies along the reach, with consequent flow acceleration and deceleration. Thus, the original hydraulic geometry relations are not dimensionally consistent, but they can be if grain size or roughness height in non-dimensional combinations with velocity (V) and unit discharge (Q) are included. Yadav, Sen, Mao and Schwanghart (2022) determined that a reduction in flow velocity and an increase in the apparent roughness length on the channel bed could be achieved as a result of the moving

Tecnología y ciencias del agua, ISSN 2007-2422, 16(4), 421-454. DOI: 10.24850/j-tyca-2025-04-10

bed grains that increase the flow resistance in bedload sediment transport.

Overreach the flow velocity limits, means causing dragging of materials, undermining of the walls and erosion of the channel bed, washing of fine material on the walls and bottom, and deformations in the section of the structure to finally inundate the floodplain and damage hydraulic works (Merchán, 2019).

One option to reduce flow velocity is by changing the roughness in the channel bed through the construction of rapids that generates a turbulent flow. For that, one of the most used methodologies for this reduction is the use of artificial roughness, which includes the incorporation of impact elements at the bottom of the channel known as rapid hydraulics structures (RHS), e.g. Radecki-Pawlik (2013) showed different real cases with a regular geometrically shaped flow director. In some cases, artificial roughness also considers removing material from a surface. In the end, the main idea is to create a two- or three-dimensional pattern that modifies the natural condition of the stream, thereby damping its excess kinetic energy. Also, as artificial roughness is considered a passive energy transfer enhancement technique, it helps to prevent riverbed erosion, stabilise bed slope and keep river channels stable, avoiding flooding conditions (Pagliara & Palermo, 2015; Takakuwa & Fukoaka, 2020; Zaborowski, Kałuza, Rybacki, & Radecki-Pawlik, 2023; Zampiron, Cameron, Stewart, Marusic, & Nikora, 2022).

It is crucial that the turbulence created by the RHS must be only in the region where the kinetic energy needs to be reduced; otherwise, it will result in negative responses, losing the fluid flow. The RHS needs to be smaller in comparison with the channel dimensions (Figure 1).

However, as there is no a specific parameter for structured roughness, Huthoff (2012) noticed that the common practice is to use roughness height values and relative roughness to assess and compare the effects of different geometries on fluid flow. Both variables are expressed in terms of Chèzy or Manning coefficients or by characteristic grain diameters of sediments in the channel.

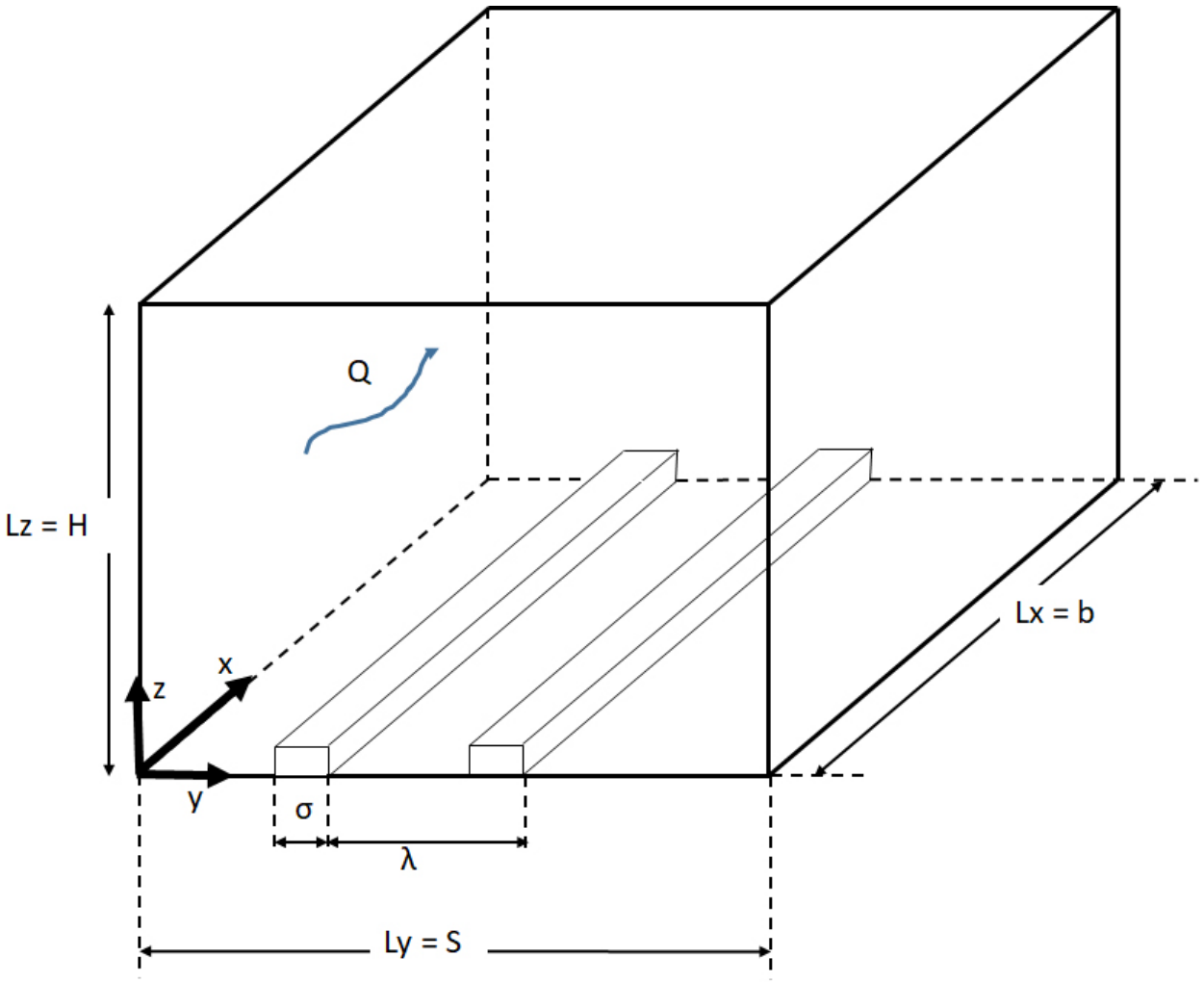

Figure 1. Geometrical parameters for transverse ribs in a channel domain. Adapted from Castro, Kim, Stroh and Lim (2021).

Andersson, Larsson, Gunnar, Burman and Andreasson (2021) have pointed out that even today, it is quite difficult to get velocity measures in situ as well as experimental results for large-scale surface roughness.

Traditionally, surface roughness considers a uniform sand grain roughness factor (k_s) for the rough surface, which creates a spatially averaged resistance for the analysed flow. This k_s requires defining an offset constant to include the shift in velocity distribution within the roughness boundary layer.

The ratio of roughness height to boundary layer thickness is frequently correlated to the transition to turbulence. Jiménez (2004) described that on turbulent flows over transverse rib-type roughness, there are two types of roughness according to the position of the ribs: d-type roughness when ribs are closely spaced such that they can sustain stable vortexes (recirculation downstream of the roughness elements) that serve to isolate the bulk flow from the roughness; and k-type roughness, which is sparser such that the flow separates at the top of the roughness element and re-attaches downstream, before reaching the next roughness element. Here, the vortexes interact with the bulk flow due to this sparse roughness, causing increased friction factors and early transition to turbulence. Also, there is a transitional roughness that occurs between these two types of roughness, because transverse rib roughness depends on the ratio of the distance between two consecutive ribs (rib pitch) and the height of the rib λ/e as shown in Figure 1.

For Coleman, Nikora, McLean and Schlicke (2007), the transitional roughness is at $\lambda/e \approx 8$ for the most predominant effect on fluid flow. Values of $\lambda/e < 5$ indicate closely spaced ribs, d-type roughness, or

Tecnología y ciencias del agua, ISSN 2007-2422, 16(4), 421-454. DOI: 10.24850/j-tyca-2025-04-10

skimming flow, while λ/e> 5 indicate isolated roughness elements, k-type roughness, or interactive flow. In the extremes where λ/e is less than 5, the roughness effect is expected to diminish the effectiveness of elements, or whether λ/e is significantly greater than 5 neither is effective since the flow retained in a first element recovers its speed until it reaches the next one and when it collides. It produces splashes and waves, affecting the flow conditions.

Researchers such as Sarkar and Dey (2010); Zhao, Wang and Lu (2001), and Andersson *et al*. (2021) continue using roughness height and relative roughness values in order to assess and compare the roughness effects with the different geometries devices on fluid flow as it was also done by Huang *et al*. (2016), and Chung, Nicholas, Schultz and Flack (2021) with their saw-tooth device (two-dimensional structured or artificial roughness), and by Coleman, Hodge and Taylor (1984) with the three-dimensional arrays of spheres, cones, and angled roughness.

In 2010, Wagner (1991) used a square geometry roughness to correlate friction factors considering height, width, and spacing of the elements, and she found that the roughness pitch is determinant in fluid flow, and they could be represented by a series of empirical formulations. Thus, the friction factor increases as roughness elements are brought closer together; i.e. higher friction factors for smaller pitch values. Also, the friction factor increases as the roughness height increases, being greater for triangular and rectangular geometries, and lower for trapezoidal roughness.

Singh and Singh (2018) showed that the key dimensionless geometrical parameters to characterise artificial roughness are:

1. Relative roughness gradient (λ/e).
2. Relative roughness height (e/B): the ratio of rib height to equivalent channel width B.
3. Angle of attack (α): the inclination of the rib with the direction of the flow, which allows transport of the induced vortexes along the rib extracting more energy.
4. Shape of roughness element: can be two-dimensional ribs or three-dimensional discrete elements. The typical shape of ribs is square, but the final shapes need to guarantee the best energy-hydraulic performance.
5. Aspect ratio: It is the ratio of channel width to channel height, crucial to defining the energy hydraulic performance.
6. Reynolds number (R_e): its influence on the flow pattern needs to be considered. As the Reynolds number increases, the vortexes intensify and appear much better defined (Sangrá-Inciarte, 1995).

Although the roughness geometry is a key parameter, its relationship with the friction factor can only be represented as a series of empirical formulations (Sun & Faghri, 2003; Wagner, 1991; Wang, Yap, & Mujumdar, 2005). Related to this, Schneider *et al*. (2015) noticed that the friction factor may be used to predict flow velocity in steep streams, particularly with low submergence of roughness elements. Krochin (1986) presented various devices of artificial roughness such as zigzag walls along the cross-section, rectangular blocks spaced a given distance, wedge-shaped walls, and bedrock or thick stones, among others.

As a result, artificial roughness only provides spatially averaged quantities, but they do not reflect the actual river dynamics. One

important point is to distinguish how the flow is transported on the rough surface due to the velocity shift when passing the obstacles. Thus, the hydraulic characteristics of the bed roughness are modified by an RHS force to include flow damping and its effect on hydraulic resistances, as well as the interaction of roughness and sedimentary density current (Kashefipour *et al*., 2018).

As bed roughness is a parameter that affects the transport mechanism and characteristics of sedimentary density current, it may be used as a suitable way for controlling the density current by decreasing flow velocity and increasing the time for settling sediment particles. Thus, the high erosive capacity of the flow is reduced, as well as a significant elevation of the water level in the curves and Mach waves, which causes the lateral spill out of the flow. For that, the study described here analyses the change of the RHS geometry from transverse ribs into ramp roughness in a right-angled channel as result of the sediment deposit. For it, the management of pitch and height ribs is crucial to reduce the speed of the flow, so that, in exchange for the channel having larger cross-sections, a more stable operation and a lower erosive capacity can be achieved. Although the relationship between the ramp roughness and the friction factor is well represented by empirical formulations, it is necessary to assess the degree of confidence that can be expected under different conditions.

Tecnología y Ciencias del Agua
OPEN ACCESS
Check for updates

Bed roughness proposal

Krochin (1986) presented different arragements to provide artificial roughness in a channel and their specific formula to define the dimensions of each roughness element. All artificial roughness models correspond to an adaptation of Wagner and Kandlikar (2012).

To increase the Chèzy roughness coefficient C of a rectangular section channel with slope S and width B, square transverse bars with side e are placed at the bottom parallel to a distance $8e$ as shown in Figure 2.

$$C = [47.5 - 1.2\,(h/e) - 0.1\,(B/h)]/1000 \qquad (1)$$

In the Equation (1), h is the water depth above the bar.

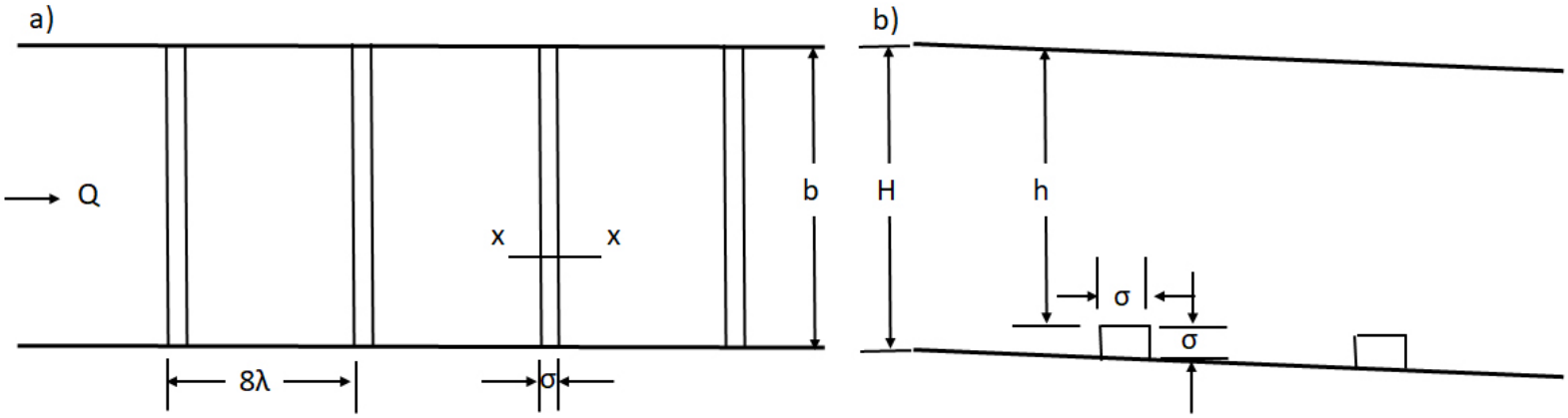

Figure 2. Transverse rib: a) plane, b) profile.

Tecnología y ciencias del agua, ISSN 2007-2422, 16(4), 421-454. DOI: 10.24850/j-tyca-2025-04-10

The Equation (1) is valid for:

$$\alpha = h/e \tag{2}$$

And:

$$\beta = B/h \tag{3}$$

Where the limited values for α and β are defined as:

$$3.5 \leq \alpha \leq 8 \tag{4}$$

$$6 \leq \beta \leq 1 \tag{5}$$

The channel energy slope S is limited as:

$$S \leq 0.15 \tag{6}$$

C roughness coefficient of Chezy formula:

$$V = C\, R^{1/2}\, S^{1/2} \tag{7}$$

Where:

V = average velocity

This channel is analysed due to its transformation into other geometries as a result of the sedimentation.

The C coefficient describes the flow velocity in channels with artificial roughness as a function of the conditions of both material and shape at the bottom, and on the wchannel wall. Also, the formulas consider the effect of the slope by introducing a correction factor for some geometries, thus the final coefficient of resistance C is calculated based on the ratios B/h and h/e , and on the depth of the flow (Saico-Bermeo & Vivar-Orellana, 2019).

The value of the velocity projected for the flow with artificial roughness, which must be less than the theoretical value corresponding to the natural roughness of the original C coefficient. R is the hydraulic radius defined in (Equation (7)) and A is the sectional area defined in (Equation (9)):

$$R = \frac{A}{b+2\,(h+e)} \tag{8}$$

$$A = b(h+e) \tag{9}$$

The discharge Q is defined in (Equation (10)):

$$Q = V\,A \tag{10}$$

Tecnología y ciencias del agua, ISSN 2007-2422, 16(4), 421-454. DOI: 10.24850/j-tyca-2025-04-10

Whether S and B are known in a channel, by selecting a value of e and choosing the one within the limits imposed in (Equation (4) and Equation (5)), it is possible to determine the value of h.

Ramp ribs

There are numerous RHS with several roughness geometries that have been studied, and each one offers some advantages over others in achieving a significant artificial roughness that provides a turbulent flow, as highlighted by Singh and Singh (2018). However, the potential sedimentation of material transported in suspension introduces an additional difficulty since it decreases the kinetic energy dissipation efficiency. Although, this condition could be challenging to occur due to the channel working in a fast regime with high velocities, it could be possible that as the velocity decreases significantly, sedimentation could occur or even the consolidation of the solids at the bottom changing the proposed roughness. This consolidation effect change can be explained by Campbell (2005), who identified that high flow resistance is associated with intermediate densities of the roughness elements since the vortex generation and the dissipation of shadow of one element are not complete before the flow meets the next element.

Also, Campbell (2005) pointed out that at high densities, a quasi-stable vortex is developed between the closely spaced in-line elements. This creates the upper limb of this vortex, which acts as a roof, and the free stream skims over the tops of the elements, as a result, a quasi-smooth flow with lower resistance is then produced (Figure 3).

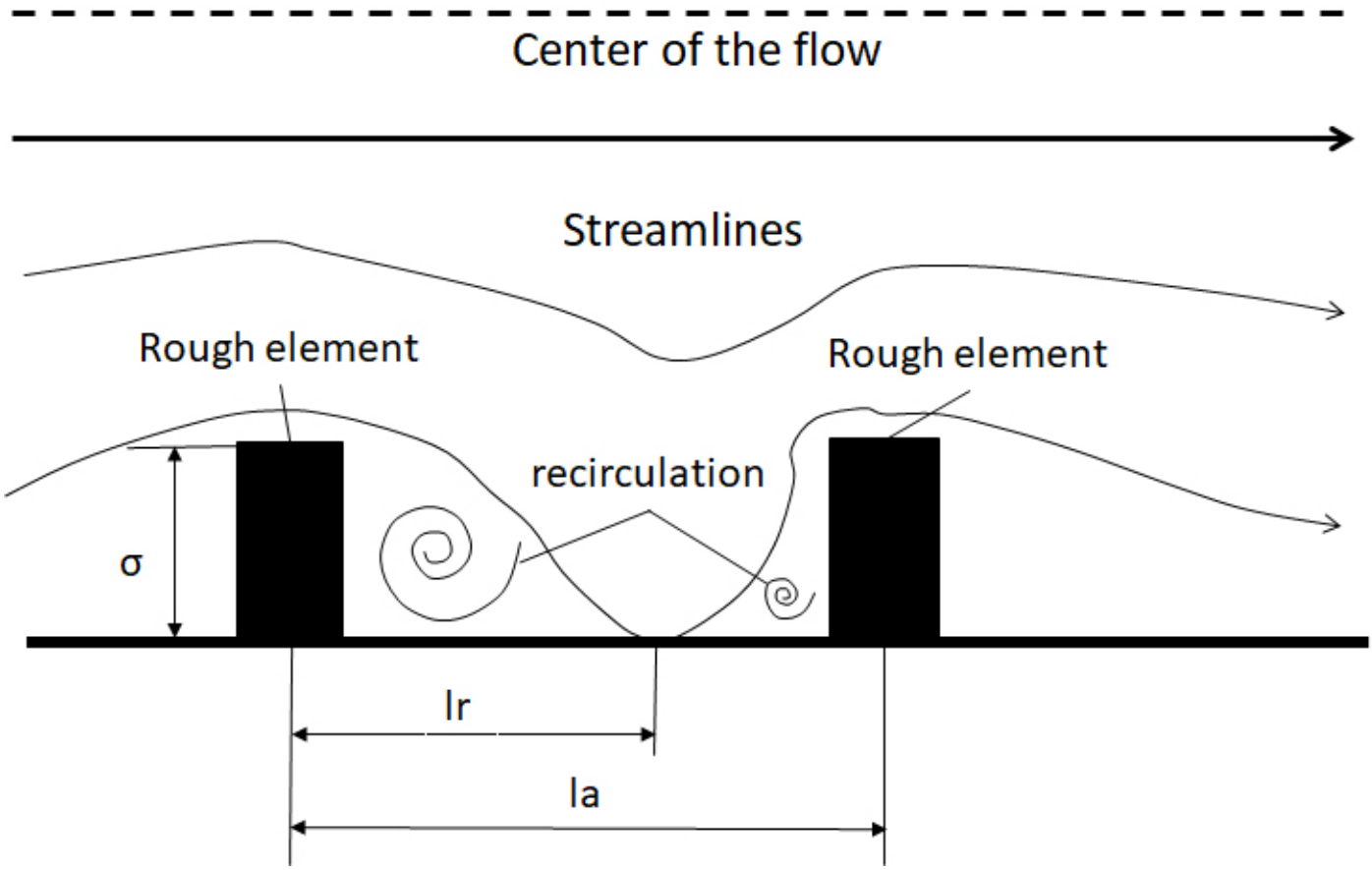

Figure 3. Streamlines for water flow through an RHS, Source: Chen *et al*. (2017).

Hassani and Reid (1990) found that when there is a reduction in bedload flux rates, an increase in flow resistance is observed, thereby increasing both roughness and energy dissipation. It was also observed that flow resistance is inversely proportional to the bedload discharge since it is implicit in the degree of energy available for moving sediment. In addition, there is bed protection generated by microforms, and as the density of the current body thickness increases, there is also a decrease

in the maximum value of velocity and an increase in in the distance of the peak value of the velocity point from the bed.

Chen *et al*. (2017) noted that the recirculation of the streamlines was mainly controlled by the angle from which the streamlines enter the rough element and by the Reynolds number (R_e). Changes in the R_e implicate modification on the flow current and shorten the distance from where the flow enters between ribs. In fact, this distance could generate recirculation vortexes quasi stables that isolate the outer flow from the roughness. The flow recirculation zone behind the rib decreases in the region before the re-joining point. Thus, the low-energy transfer region behind the rib is reduced, which results in an enhancement of the overall flow velocity (Figure 4).

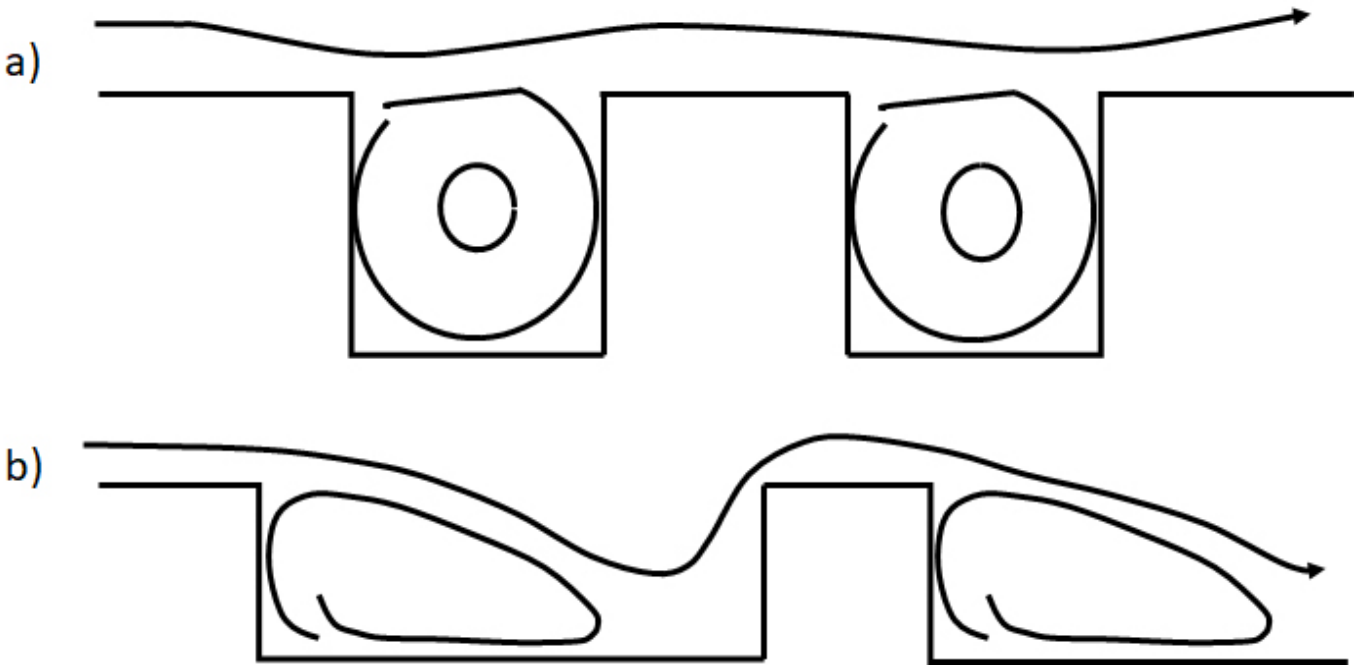

Figure 4. Geometry of a) d-type, and b) k-type rib walls. Source: Andersson *et al*. (2021).

Andersson *et al*. (2021) showed a natural modification of the geometry roughness based on the constructive simplicity of transverse ribs, by introducing a slope, ramps are created by the sediment consolidation. This geometry (Figure 5) can be associated with the one proposed by Huthoff (2012).

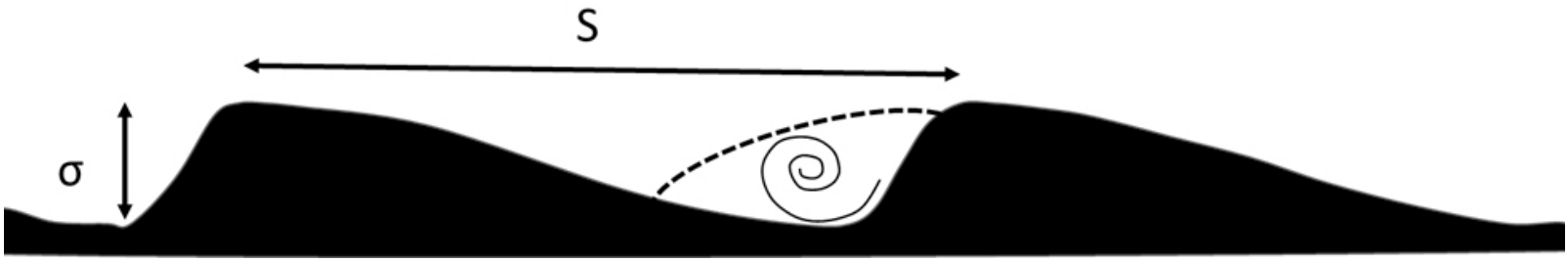

Figure 5. Roughness geometry for the proposal ramps ribs. Adapted from Huthoff (2012).

The geometry proposed in this paper (Figure 6) has a slope (S_R) different to the channel slope S as well as modifications in the width of the bottom channel (B), the transverse ribs with height (e) and the separation between each geometry (λ) (Sánchez-B., Gracia-S., & Franco, 2000).

Tecnología y ciencias del agua, ISSN 2007-2422, 16(4), 421-454. DOI: 10.24850/j-tyca-2025-04-10

Tecnología y Ciencias del Agua
OPEN ACCESS
Check for updates

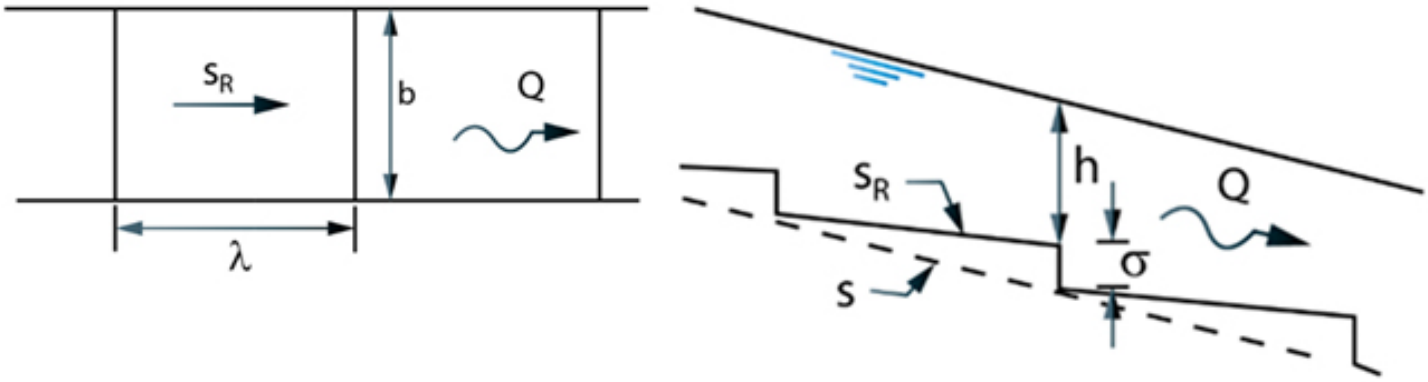

Figure 6. Ramps' roughness: a) plane and b) profile.

When a discharge Q, the difference in level between the free surface of the water and the upper end of the height rib is h. The spacing between the super-elevations of the steps is λ equal to $8e$. (Equation (4)) and (Equation (5)) are applied, but the limited values for σ_* and β_* are redefined as:

$$3 \leq \alpha \leq 7 \tag{11}$$

$$1 \leq \beta \leq 6 \tag{12}$$

For energy slope S of the channel the friction coefficient is:

$$C = (3.3 + 32\, S^{\frac{1}{4}} + 10\, \beta^{\frac{1}{9}} - 0.67\alpha)/1000 \tag{13}$$

In this case the radius and hydraulic area are obtained with equations (14) and (15):

$$R = \frac{A}{b+2\,(h + e/2)} \tag{14}$$

$$A = b(h + e\ /\ 2) \tag{15}$$

Mathematical criteria to compute ramp roughness

For the design of a channel with artificial roughness, the dimensions and slope of the channel must first be defined, as well as the flow velocity of the channel without roughness, and a proposed initial flow velocity value to be reached (less than the observed in the channel).

Therefore, for a channel with artificial roughness, it is proposed to express the discharge Q as a potential function of the dimensionless variables h/e, B/h and S as:

$$Q = a\,(h/e)^b\,(B/h)^c\,S^d \tag{16}$$

In order to know the a, b, c, d constants in a channel, it is necessary to select N sets of values for $F_r, (h/e), (B/e)$ and S, observing the limits imposed by Equation 4 to Equation (6). The constant a has the same units as the flow rate; other constants b, c and d are dimensionless.

Tecnología y ciencias del agua, ISSN 2007-2422, 16(4), 421-454. DOI: 10.24850/j-tyca-2025-04-10

Whether $w = \ln Q$, $x = ln\,(h/e)$, $y = ln(B/e)$ and $z = ln\,S$, according to the least squares method (Zienkiewicsz, Taylor, & Zhu, 2013), the system of linear equations formed is (Equation (17)):

$$\begin{pmatrix} N & \Sigma x & \Sigma y & \Sigma z \\ \Sigma x & \Sigma x^2 & \Sigma xy & \Sigma xz \\ \Sigma y & \Sigma xy & \Sigma y^2 & \Sigma yz \\ \Sigma z & \Sigma xz & \Sigma yz & \Sigma z^2 \end{pmatrix} \begin{pmatrix} a \\ b \\ c \\ d \end{pmatrix} = \begin{pmatrix} \Sigma w \\ \Sigma xw \\ \Sigma yw \\ \Sigma zw \end{pmatrix} \quad (17)$$

The solution of this system corresponds to values of a, b, c and d required to compute Q values in (Equation (16)) for each one of the N sets of values.

Set values results and discussion

This section presents the application results of the theoretical model, which is used to understand the effects of each variable prior to the production of the roughness of the ramps. Special attention needs to be focused on Kashefipour *et al*. (2018) findings, which identified that increasing bed slope generally increases the maximum velocity but reduces depth.

Additionally, in sedimentary density fluids, when the density is increased, the flow velocity also increases due to the difference between densities. Thus, for a proposed channel with a width bottom of 6 m, it was considered in total, 27 N set values for Q, e, h/e, B/h and S (Table 1).

Table 1. Selected values of some elements of the channel.

Set	e (m)	h (m)	h/e	B/h	S	Q($m^3 \cdot s^{-1}$)
1	0.280	1.960	7.000	3.061	0.15	181.711
2	0.280	1.610	5.750	3.727	0.150	138.199
3	0.280	1.010	3.600	5.952	0.150	73.673
4	0.380	2.660	7.000	2.256	0.150	271.680
5	0.380	2.180	5.750	2.746	0.150	207.995
6	0.380	1.330	3.500	4.511	0.150	108.520
7	0.480	3.360	7.000	1.786	0.150	366.609
8	0.480	2.760	5.750	2.174	0.150	282.131
9	0.480	1.680	3.500	3.571	0.150	149.051
10	0.280	1.960	7.000	3.061	0.100	158.565
11	0.280	1.610	5.750	3.727	0.100	120.304
12	0.280	1.010	3.600	5.952	0.100	63.870
13	0.380	2.660	7.000	2.256	0.100	237.283
14	0.380	2.180	5.750	2.746	0.100	181.214
15	0.380	1.330	3.500	4.511	0.100	94.134
16	0.480	3.360	7.000	1.786	0.100	320.407
17	0.480	2.760	5.750	2.174	0.100	245.962
18	0.480	1.680	3.500	3.571	0.100	129.367
19	0.280	1.960	7.000	3.061	0.050	124.929
20	0.280	1.610	5.750	3.727	0.050	94.380
21	0.280	1.010	3.600	5.952	0.050	49.746
22	0.380	2.660	7.000	2.256	0.050	187.242
23	0.380	2.180	5.750	2.746	0.050	142.376
24	0.380	1.330	3.500	4.511	0.050	73.391
25	0.480	3.360	7.000	1.786	0.050	253.139
26	0.480	2.760	5.750	2.174	0.050	193.463
27	0.480	1.680	3.500	3.571	0.050	100.963

Tecnología y ciencias del agua, ISSN 2007-2422, 16(4), 421-454. DOI: 10.24850/j-tyca-2025-04-10

Based on the data in Table 1, the following values for the dimension and dimensionless parameters were derived, where Q was computed using Equation (13) to Equation (15).

The solution to the matrix of least squares in Equation 17 achieves a $\widetilde{Q}$ value.

$$a = 1566.8767$$

$$b = -0.0030$$

$$c = -1.3386$$

$$d = 0.3471$$

Discharge $\widetilde{\mathrm{Q}}$ in a bottom channel of 6 m is convincingly reliable according to the following expression:

$$\widetilde{\mathrm{Q}} = 1566.8767(\mathrm{B/h})^{-1.3386}(\mathrm{h/e})^{-0.0030}\ \mathrm{S}^{0.3471} \tag{18}$$

The computation unexplained variation $\mathrm{V_{NE}} = \sum_{i=1}^{27}(\widetilde{\mathrm{Q}} - \mathrm{Q})^2 = 64.52$

The total variation is $\mathrm{V_T} = \sum_{i=1}^{27}(\widetilde{\mathrm{Q}} - \overline{\mathrm{Q}})^2 = 914334.36$

The adjusted coefficient of determination is

$$\mathrm{D}^2 = 1 - \frac{\dfrac{\mathrm{V_{NE}}}{[\mathrm{n} - (\mathrm{p}+1)]}}{\dfrac{\mathrm{V_T}}{[\mathrm{n}-1]}} = 1 - \frac{\dfrac{64.52}{[27-(3+1)]}}{\dfrac{914334.36}{[26]}} = 0.999$$

Where:

n = number of sets

p = number of variables explained, in this case 3.

Knowing the discharge $\tilde{Q}$, B and energy slope S (Equation (18)), for each value of e there is a value for h. To validate these results, it is useful to verify that the limit values for α and β (in Equation (4) and Equation (5)) are observed. As the roughness height (h / e) is known, it is possible to estimate the Chèzy or Manning roughness coefficient.

In this case using h, the hydraulic area is obtained with Equation (15) for a channel of rectangular section, width bottom B, and slope S, thus average velocity of the water is:

$$V = \frac{Q}{A} \tag{19}$$

The hydraulic radius is calculated with Equation (14), the Chèzy and Manning roughness coefficients are:

$$C = \frac{V}{R^{1/2} S^{1/2}} \tag{20}$$

$$n = \frac{R^{2/3} S^{1/2}}{V} \tag{21}$$

The roughness coefficients of Chèzy and the Manning coefficient are present in Table 2 for each 27 N set of data used.

Tecnología y Ciencias del Agua
OPEN ACCESS
Check for updates

Table 2. Chèzy and Manning Coefficient, *n*, for ramps ribs.

Set	Q (m^3/s)	S	e (m)	h (m)	A (m^2)	R (m)	V (m/s)	C Chezy ($m^{1/2}/s$)	n Manning ($s/m^{1/3}$)
1	181.7110	0.1500	0.2800	1.9600	12.6000	1.2353	14.4215	33.5027	0.0309
2	138.1990	0.1500	0.2800	1.6100	10.5000	1.1053	13.1618	32.3249	0.0315
3	73.6730	0.1500	0.2800	1.0100	6.9000	0.8313	10.6772	30.2363	0.0321
4	271.6800	0.1500	0.3800	2.6600	17.1000	1.4615	15.8877	33.9321	0.0314
5	207.9950	0.1500	0.3800	2.1800	14.2200	1.3240	14.6269	32.8216	0.0319
6	108.5200	0.1500	0.3800	1.3300	9.1200	1.0088	11.8991	30.5884	0.0327
7	366.6090	0.1500	0.4800	3.3600	21.6000	1.6364	16.9726	34.2581	0.0317
8	282.1310	0.1500	0.4800	2.7600	18.0000	1.5000	15.6739	33.0436	0.0324
9	149.0510	0.1500	0.4800	1.6800	11.5200	1.1707	12.9385	30.8751	0.0333
10	158.5650	0.1000	0.2800	1.9600	12.6000	1.2353	12.5845	35.8057	0.0289
11	120.3040	0.1000	0.2800	1.6100	10.5000	1.1053	11.4575	34.4634	0.0295
12	63.8700	0.1000	0.2800	1.0100	6.9000	0.8313	9.2565	32.1042	0.0302
13	237.2830	0.1000	0.3800	2.6600	17.1000	1.4615	13.8762	36.2966	0.0293
14	181.2140	0.1000	0.3800	2.1800	14.2200	1.3240	12.7436	35.0223	0.0299
15	94.1340	0.1000	0.3800	1.3300	9.1200	1.0088	10.3217	32.4966	0.0308
16	320.4070	0.1000	0.4800	3.3600	21.6000	1.6364	14.8337	36.6698	0.0296
17	245.9620	0.1000	0.4800	2.7600	18.0000	1.5000	13.6646	35.2817	0.0303
18	129.3670	0.1000	0.4800	1.6800	11.5200	1.1707	11.2298	32.8203	0.0313
19	124.9290	0.0500	0.2800	1.9600	12.6000	1.2353	9.9150	39.8954	0.0260
20	94.3800	0.0500	0.2800	1.6100	10.5000	1.1053	8.9886	38.2360	0.0266
21	49.7460	0.0500	0.2800	1.0100	6.9000	0.8313	7.2096	35.3621	0.0274
22	187.2420	0.0500	0.3800	2.6600	17.1000	1.4615	10.9498	40.5058	0.0263
23	142.3760	0.0500	0.3800	2.1800	14.2200	1.3240	10.0124	38.9139	0.0269
24	73.3910	0.0500	0.3800	1.3300	9.1200	1.0088	8.0473	35.8302	0.0280
25	253.1390	0.0500	0.4800	3.3600	21.6000	1.6364	11.7194	40.9714	0.0265
26	193.4630	0.0500	0.4800	2.7600	18.0000	1.5000	10.7479	39.2459	0.0273
27	100.9630	0.0500	0.4800	1.6800	11.5200	1.1707	8.7641	36.2240	0.0283

Tecnología y ciencias del agua, ISSN 2007-2422, 16(4), 421-454. DOI: 10.24850/j-tyca-2025-04-10

Channel numerical model to test equations for ramp ribs

The artificial roughness in equations Chèzy and Manning transverse, and ramps ribs was studied by applying Equation (18) and Equation (20) controlling height (h), pitch, side section (almost square,e), and slope (S). The channel has a rectangular section with a width B of 6.0 m and a slope S of 0.15. The channel was excavated in the rock, thus the height difference between the bottom channel and the free surface h is 3.2 m. The flow of water has a discharge of Q = 95 $m^3 \cdot s^{-1}$.

- Rectangular section channel without artificial roughness. The lined channel without artificial roughness geometry has a roughness coefficient of n = 0.015. As, Q = 95 $m^3 \cdot s^{-1}$, the depth h = 0.822 m, the average velocity V=19.262 $m \cdot s^{-1}$ and the Fr = 6.7831.
- Rectangular section channel with transverse ribs. To reduce the velocity in the channel, artificial roughness was used installing transverse ribs with the characteristics of width B = 6 m, and side section e is 0.28m, slope S = 0.15 and discharge Q = 95 $m^3 \cdot s^{-1}$. Substituting these values, the h value is 0.822 m, the velocity is 19.262 m$\cdot s{-}^{1}$, the Chèzy coefficient is 61.9161, and the F_r number is 6.7831.
- Rectangular section channel with ramps. Once transverse ribs change their behavior due to sediment deposition between (8e), it is assumed that the geometry could now work as ramps. The moment when this condition takes place it is highly variable due to the physic-chemical

Tecnología y ciencias del agua, ISSN 2007-2422, 16(4), 421-454. DOI: 10.24850/j-tyca-2025-04-10

sediment composition. Thus, the flow operation under this condition is modified to e = 0.28 m and h = 1.213 m, if the free surface is $h + e/2$ = 1.353 m less than 3.20 m, this means water did not spill out and the average velocity as F_r number can be reduced from the geometry without RHS to 3.2121. The n value calculated is 0.0316 $s\, m^{-1/3}$.

The theory presented here involves concepts from the phenomenological theory of turbulence and fluid mechanics, thus:

- *For the original condition*, the water depth is small, the velocity is very high, as well as the Froude number, with very low roughness.
- *For the transverse rib condition*, water depth increases, whereas velocity decreases, as well as the Froude number, but the roughness coefficient increases.
- *For the ramp condition*, water depth decreases again, velocity is higher than in transverse ribs geometry, as well as the Fr number, but n decreases.

The flow depth in the coefficient of Manning's equation on the transverse ribs and ramps indicates that the flow is above the roughness elements. Thus, the ramps formed with the sediment really modify the flow operation provided with transverse ribs. In the numerical exercise, it is evident that velocity adjustment is significant from 19.262 $m{\cdot}s^{-1}$ to 11.072 $m{\cdot}s^{-1}$, which corresponds to a decrement of 57 %.

Although it was considered that the vortexes generated between ribs sometimes did not affect the prevailing turbulence flow, this recirculation in time is the cause of sediment deposits from sediment load fluids, which can be placed at any time or even not at all. Thus, the drag

coefficient needs to include the shape effects of the obstruction (streamlining), the submergence ratio and the effects of the vortexes for the two dimensions of roughness elements with frontal width and height.

As sediment consolidation depends on the type of sediment transported, bed roughness remains useful, although a little less effective. In addition, to validate the results obtained with a ramp geometry, the solid material should not be removed for an extended period so that it can be cemented; typical examples of this are soil mixtures of sand and clay (Dankers, Sills, & Winterwerp, 2008; van Rijn & Barth, 2018). According to the data obtained, for flows with lower discharge, the velocity of the water could remove the particles of sand of regular size and lime – clays, but it will be in function of the consolidation degree of the deposited material.

Conclusions

In general, the RHS are functions of variables such as material, structure, distribution, and streamline reattachment length (vortex). Looking at the geometry, it can be confirmed that transverse ribs roughness in a rectangular section of lined channels shows a more stable water flow within a wider working range, however, this option is more expensive and less resistant to wear.

On the contrary, when ramps are created as a result of the natural modification to the transverse ribs due to sediment consolidation, this geometry is less expensive and more resistant to wear. Therefore, it is highly recommended to reduce water velocities, which tend to increase as well as the Froude number. In practice, the formation of ramps is

Tecnología y ciencias del agua, ISSN 2007-2422, 16(4), 421-454. DOI: 10.24850/j-tyca-2025-04-10

frequent, but it will depend on the amount of fine material (silt – clay) and its consolidation, and also to the variation of speeds over these structures.

It is essential to consider that the channel designs are made for the maximum flow rate with a relatively low probability of occurrence; thus, with the RHS, lower fluid rates are expected, and the roughness element wear can be attenuated. Also, the results obtained in the calculation examples demonstrated that when the designs are made for Froude numbers less than 1.5, the deposit increases, respecting the unevenness between the natural terrain and the channel bottom, free embankments are available, consequently as flood protection.

Finally, installing a ramp's geometry roughness seems to be the best option to reduce water flow velocity by increasing the bottom roughness in the channel. Howeverit is necessary to take special attention to the consolidation of the sediment deposit since solid deposits will continue, and a further transformation of the ramps could be achieved till modify the original rib elements.

Acknowledgments

Thanks to Liliana Marrufo Vázquez for her helpful discussions on an earlier draft of this manuscript.

References

Andersson, L., Larsson, I., Gunnar, J. H. I., Burman, A., & Andreasson, P. (2021). Localized roughness effects in non-uniform hydraulic waterways. *Journal of Hydraulic Research*, 59(1), 100-108. DOI: 10.1080/00221686.2020.1744744

Campbell, L. J. (2005). *Double-averaged open-channel flow over regular rough beds.* (Ph.D. thesis, School of Engineering, University of Aberdeen, Aberdeen). Recovered from https://www.semanticscholar.org/paper/Double-averaged-open-channel-flow-over-regular-beds-Campbell/12c71cd21584c973b1bdcdbd166df75e0d2b86cd

Castro, I. P., Kim, J. W., Stroh, A., & Lim, H. C. (2021). Channel flow with large longitudinal ribs. *Journal of Fluid Mechanics*, 915, A92. DOI: 10.1017/jfm.2021.110

Chanson, H. (1999). *The hydraulics of open channel flow: An introduction*. London, UK: Butterworth-Heinemann Eds.

Chen, Z., Qian, J., Zhan, H., Zhou, Z., Wang, J., & Tan, Y. (2017). Effect of roughness on water flow through a synthetic single rough fracture. *Environmental Earth Sciences*, 76(186), 2-17. DOI: 10.1007/s12665-017-6470-7

Chung, D., Nicholas, H., Schultz, M. P., & Flack, K. A. (2021). Predicting the drag of rough surfaces. *Annual Review of Fluid Mechanics*, 53, 439-471. DOI: 10.1146/annurev-fluid-062520115127

Coleman, H. W., Hodge, B. K., & Taylor, R. P. (1984). A re-evaluation of schlichting's surface roughness experiment. *Journal of Fluids Engineering*, 106(1), 60-65. DOI: 10.1115/1.3242406

Coleman, S. E., Nikora, V. I., McLean, S. R., & Schlicke, E. (2007). Spatially averaged turbulent flow over square ribs. *Journal of Engineering Mechanics*, 133(2), 194-204. DOI: 10.1061/(ASCE)0733-9399133:2(194)

Dankers, P. J. T., Sills, G. C., & Winterwerp, J. C. (2008). Chapter 18. On the hindered settling of highly concentrated mud-sand mixtures. In: Kusuda, T., Yamanishi, H., Spearman, J., & Gailani, J. Z. (eds.). *Sediment and ecohydraulics* (pp. 255-274). Amsterdam, Netherlands: INTERCOH 2005, Elsevier B. V. DOI: 10.1016/S1568-2692(08)80020-4

Ferguson, R. I. (2022). *Reach-scale flow resistance*. Durham, UK: Elsevier Inc. DOI: 10.1016/B978-0-12-409548-9.09386-6

Hassani, M. A., & Reid, I. (1990). The influence of microform bed roughness elements on flow and sediment transport in gravel-bed rivers. *Earth Surface Processes and Landforms*, 15(8), 739-750. DOI: 10.1002/esp.3290150807

Huang, G., Simoëns, S., Vinkovic, I., Le Ribault, C., Dupont, S., & Bergametti,G. (2016). Law-of-the-wall in a boundary-layer over regularly distributed roughness elements. *Journal of Turbulence*, 17(5), 518-541. DOI: 10.1080/14685248.2016.1139121

Huthoff, F. (2012). Theory for flow resistance caused by submerged roughness elements. *Journal of Hydraulic Research*, 50(1), 10-17. DOI: 10.1080/00221686.2011.636635

Jiménez, J. (2004). Turbulent flows over rough walls. *Annual Review of Fluid Mechanics*, 36, 173-196. DOI: 10.1146/annurev.fluid.36.050802.122103

Kashefipour, S. M., Daryaee, M., & Ghomeshi, M. (2018). Effect of bed roughness on velocity profile and water entrainment in a sedimentary density current. *Canadian Journal of Civil Engineering*, 45, 9-17. DOI: 10.1139/cjce-2016-0490

Krochin, S. (1986). *Diseño hidráulico*. Quito, Ecuador: Escuela Politécnica Nacional.

Merchán, P. N. (2019). *Simulación numérica experimental de un canal con un nuevo modelo de rugosidad artificial* (B. S. E. thesis). Facultad de Ingeniería, Universidad de Cuenca, Cuenca, Ecuador. Recovered from http://dspace.ucuenca.edu.ec/handle/123456789/32054

Pagliara, S., & Palermo, M. (2015) Hydraulic jumps on rough and smooth beds: Aggregate approach for horizontal and adverse-sloped beds. *Journal of Hydraulic Research*, 53(2), 243-252. DOI: 10.1080/00221686.2015.1017778

Radecki-Pawlik, A. (2013). On using artificial rapid hydraulic structures (RHS) within mountain stream channels: Some exploitation and hydraulic problems. In: Rowiński, P. (ed.). *Experimental and Computational Solutions of Hydraulic Problems*. Berlin, Germany: GeoPlanet: Earth and Planetary Sciences, Springer. DOI: 10.1007/978-3-642-30209-1_6

Saico-Bermeo, V. D., & Vivar-Orellana, R. A. (2019). *Evaluación de métodos de diseño para conductos con rugosidad artificial mediante experimentación en modelo físico*. (B. S. E. thesis). Facultad de Ingeniería, Universidad de Cuenca, Cuenca, Ecuador. Recovered from http://dspace.ucuenca.edu.ec/handle/123456789/32576

Sangrá-Inciarte, P. (1995). *Perturbación de un flujo geofísico por un obstáculo. Aplicación a la isla de Gran Canaria* (Ph.D. thesis). Departamento de Física, Universidad de las Palmas de Gran Canaria, España. Recovered from https://accedacris.ulpgc.es/handle/10553/1913

Sarkar, S., & Dey, S. (2010). Double averaging turbulence characteristics in flows over a gravel bed. *Journal of Hydraulic Research*, 48(6), 801–809. DOI: 10.1080/00221686.2010.526764.430

Schneider, J. M., Rickenmann, D., Turowski, J. M., & Kirchner, J. W. (2015). Self-adjustment of stream bed roughness and flow velocity in a steep mountain channel. *Water Resources Research*, 51, 7838-7859. DOI: 10.1002/2015WR016934

Singh, I., & Singh, S. (2018). A review of artificial roughness geometries employed in solar air heaters. *Renewable and Sustainable Energy Reviews*, 92, 405-425 DOI: 10.1016/j.rser.2018.04.108

Sun, H., & Faghri, M. (2003). Effect of surface roughness on nitrogen flow in a microchannel using the direct simulation Monte Carlo method. *Numerical Heat Transfer Applications*, 43(1), 1-8. DOI: 10.1080/10407780307302

Sánchez-B, J. L., Gracia-S., J., & Franco, V. (2000). Critical review of equations to determine the effect of artificial roughness in a channel with steep slopes. *Dam Enginnering,* 11(2), 89-109.

Takakuwa, Y., & Fukuoka, S. (2020). Three-dimensional flow structures of straight rough-bed channels with different aspect ratios. In: Uijttewaal *et al*. (eds.). *River Flow 2020.* Abingdon-on-Thames, UK: Taylor & Francis Group. DOI: 10.1201/b22619-9

Tollner, E. W. (2021). *Open channel design: Fundamentals and applications*. Oxford, UK: John Wiley & Sons Ltd. DOI: 10.1002/9781119664338

van Rijn, L. C., & Barth, R. (2018). Settling and consolidation of soft mud-sand layers. *Journal of Waterway, Port, Coastal, and Ocean Engineering*, 145(1), 04018028. DOI: 10.1061/(ASCE)WW.1943-5460.0000483

Wagner, R., & Kandlikar, S. G. (2012). Effects of structured roughness on fluid flow at the microscale level. *Heat Transfer Engineering*, 33(6), 483-493. DOI: 10.1080/01457632.2012.624850

Wagner, R. N. (1991). *Effects of structured roughness on fluid flow at the microscale level*. (M. S. thesis). Rochester, USA: Rochester Institute of Technology. Recovered from https://scholarworks.rit.edu/theses/5893/

Wang, X. Q., Yap, C., & Mujumdar, A. S. (2005). Effects of two-dimensional roughness in flow in microchannels. *Journal of Electronic Packaging*, 127(3), 357-361 DOI: 10.1115/1.1997164

Yadav, A., Sen, S., Mao, L., & Schwanghart, W. (2022) Evaluation of flow resistance equations for high gradient rivers using geometric standard deviation of bed material. *Journal of Hydrology*, 605, 127292. DOI: 10.1016/j.jhydrol.2021.127292

Yochum, S. E., Bledsoe, B. P., David, G. C. L., & Wohl, E. (2012). Velocity prediction in high-gradient channels. *Journal of Hydrology*, 424-425, 84-98. DOI: 10.1016/j.jhydrol.2011.12.031

Zaborowski, S., Kałuza, T., Rybacki, M., & Radecki-Pawlik, A. (2023) Influence of river channel deflector hydraulic structures on lowland river roughness coefficient values: The Flinta river, Wielkopolska Province, Poland. *Ecohydrology & Hydrobiology*, 23, 79-97. DOI: 10.1016/j.ecohyd.2022.10.002

Zampiron, A., Cameron, S. M., Stewart, M.T., Marusic, I., & Nikora, V. I. (2023) Flow development in rough-bed open channels: mean velocities, turbulence statistics, velocity spectra, and secondary currents. *Journal of Hydraulic Research*, 61(1), 133-144. DOI: 10.1080/00221686.2022.2132311

Zhao, Y., Wang, G. C., & Lu, T. M. (2001). Characterization of amorphous and crystalline rough surface: Principles and applications. Experimental Methods in the Physical Sciences. In: Celotta, R., & Lucatorto, T. (eds.). *Book Series* (Vol. 37) (pp. 417). Cambridge, USA: Academic Press.

Zienkiewicsz, O. C., Taylor, R. L., & Zhu, J. Z. (2013). Variational forms and finite element approximation: 1-d problems. In: Zienkiewicz, J. Z. Z. O. C., & Taylor, R. L. (eds.). *The finite element method: Its basis and fundamentals*. Exeter, UK: Elsevier. DOI: 10.1016/B978-1-85617-633-0.00004-6